

PROCEEDINGS OF SPIE

[SPIDigitalLibrary.org/conference-proceedings-of-spie](https://spiedigitallibrary.org/conference-proceedings-of-spie)

First results of EUV-scanner compatibility tests performed on novel 'high-NA' reticle absorber materials

Stortelder, Jetske, Ebeling, Rob, Rijnsent, Corné, van Putten, Michel, de Rooij-Lohmann, Véronique, et al.

Jetske Stortelder, Rob Ebeling, Corné Rijnsent, Michel van Putten, Véronique de Rooij-Lohmann, Maximilian Smit, Arnold Storm, Norbert Koster, Henk Lensen, Vicky Philipsen, Karl Opsomer, Devesh Thakare, Torsten Feigl, Philipp Naujok, "First results of EUV-scanner compatibility tests performed on novel 'high-NA' reticle absorber materials," Proc. SPIE 11854, International Conference on Extreme Ultraviolet Lithography 2021, 1185414 (12 October 2021); doi: 10.1117/12.2600928

SPIE.

Event: SPIE Photomask Technology + EUV Lithography, 2021, Online Only

First results of EUV-scanner compatibility tests performed on novel 'high-NA' reticle absorber materials

Jetske Stortelder^{*a}, Rob Ebeling^a, Corné Rijnsent^a, Michel van Putten^a, Véronique de Rooij-Lohmann^a, Maximilian Smit^a, Arnold Storm^a, Norbert Koster^a, Henk Lensen^a, Vicky Philipsen^b, Karl Opsomer^b, Devesh Thakare^b, Torsten Feigl^c, Philipp Naujok^c

^aTNO, Stieltjesweg 1, 2628 CK Delft, The Netherlands;

^bimec, Kapeldreef 75, B-3001 Leuven, Belgium;

^coptiX fab GmbH, Hans-Knoell-Strasse 6, 07745 Jena, Germany

ABSTRACT

Novel reticle absorber materials are required for high-NA EUV lithography. TNO and ASML developed an assessment for the compatibility of novel high-NA reticle absorber materials with conditions that mimic the EUV scanner environment^[1]. Four candidate reticle absorber materials were evaluated, TaCo, RuTa, PtMo and Pt₂Mo alloys, in a joint research program. For the compatibility tests, dedicated samples with silicon wafer substrates were fabricated. The silicon wafers were coated with a Mo-Si multilayer coating, followed by a Ru capping layer and finally the absorber material.

Chemical outgassing tests, in presence of hydrogen radicals, did not show chemical outgassing for the TaCo and PtMo alloys. RuTa and Pt₂Mo alloys were not tested, based upon their elemental composition chemical outgassing is not expected. Next, all four materials were exposed in a hydrogen plasma resistance test equivalent to an EUV exposure of at least 250 thousand wafers^{**} in the EUV scanner. No plasma-induced defects, like blistering or delamination, were found that were related to the intrinsic absorber properties.

The RuTa and PtMo alloys were selected for EUV exposure in the EBL2 facility at TNO. Both materials were exposed to an 9.6 kJ/mm² EUV peak dose at an EUV peak intensity of 450 mW/mm² in a hydrogen environment. This EBL2 EUV exposure of 6 hours represents about 1-2 months of EUV dose (at least 150 thousand wafers) in a NXE or EXE scanner with a 300 W source. Both materials showed good performance during EUV exposure. Relevant surface defects and chemical outgassing were not observed. The few observed blisters in the low EUV intensity areas are likely provoked by particle contamination or coating defects.

All four absorber materials, TaCo, RuTa, PtMo and Pt₂Mo alloys performed well in the compatibility tests that were executed. Not all compatibility tests could be performed on each absorber material within the scope of our research program. Further testing would be needed to complete the compatibility assessment, including an EUV exposure on a patterned reticle.

Keywords: reticle, mask, absorber, EUV, optics lifetime, contamination control, accelerated life time tests, high-NA

*jetske.stortelder@tno.nl; www.tno.nl

**All wafer estimations in this publication are for 30 mJ/cm² resist sensitivity in a NXE or EXE system with a 300 W source. The actual number of wafers depends on the used EUV scanner settings.

International Conference on Extreme Ultraviolet Lithography 2021, edited by Kurt G. Ronse, Patrick P. Naulleau, Paolo A. Gargini, Toshiro Itani, Eric Hendrickx, Proc. of SPIE Vol. 11854, 1185414 · © 2021 SPIE · CCC code: 0277-786X/21/\$21 · doi: 10.1117/12.2600928

Proc. of SPIE Vol. 11854 1185414-1

1. INTRODUCTION

Novel reticle absorber materials are studied for use in high-NA EUV scanners^[2-6] to optimize imaging performance. The candidate reticle absorber materials need to meet high standards with respect to optical performance, pattern etch and repair, pattern quality, cleaning durability, absorber (reticle) lifetime and compatibility with the EUV scanner environment. In this publication four absorber materials were tested, RuTa, TaCo, PtMo, and Pt₂Mo alloys. These materials showed promising results in previous studies^[3,4], for example on optical constants and cleaning durability, and therefore were selected for compatibility testing. RuTa, PtMo, Pt₂Mo alloys have an extinction coefficient (k) close to that of the currently used Ta-based absorber at 13.5 nm wavelength. The refraction coefficient (n) of these alloys is lower and therefore these alloys are considered for Attenuated Phase-Shift masks (attPSM). TaCo has a higher extinction coefficient and a refraction coefficient that is closer to that of vacuum and is therefore an absorber candidate for binary (high- k) masks.

The samples tested in this publication were deposited by magnetron sputtering at imec and optiX fab. For the tests, dedicated test samples with silicon wafers were fabricated. The silicon wafers were coated with a Mo-Si multilayer coating, followed by a Ru capping layer and finally the absorber material. Note that the naming convention of the materials (RuTa, TaCo, PtMo, Pt₂Mo) does not necessarily represent the actual stoichiometry.

The compatibility assessment is shown schematically in Figure 1. The tests in part 1 might also be performed parallel or in a different order. When an absorber material performs well in a test, it continues to the next test. If it does not perform well, it is considered not compatible with the EUV scanner environment and further testing is stopped. Not all compatibility tests could be performed on each absorber material within the scope of our research program, therefore a selection of materials was made for each test. In the conclusions you can find an overview of all test results in Table 1.

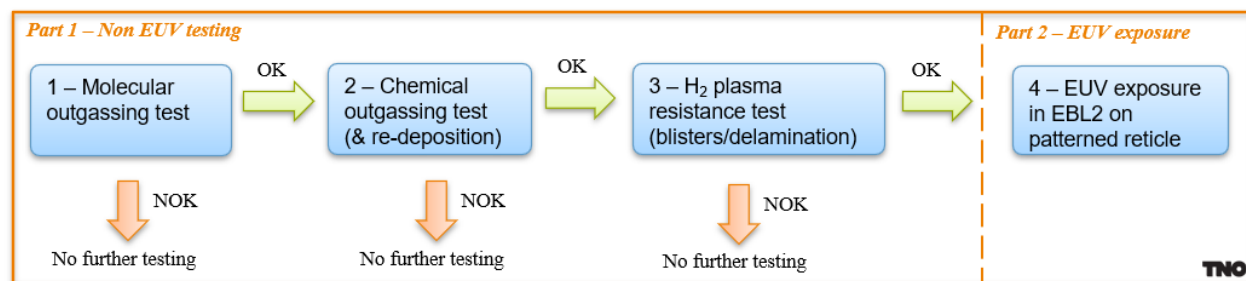


Figure 1: Simplified flowchart for the compatibility assessment of novel reticle absorber materials for use in the EUV scanner.

2. COMPATIBILITY ASSESSMENT – PART 1 – NON-EUV TESTS

The first part of the assessment tests materials in different environments without EUV. The environments used are high vacuum, hydrogen radicals and hydrogen plasma. These environments test the absorber material on molecular outgassing, chemical outgassing and re-deposition of absorber material and hydrogen plasma resistance of the absorber. Materials with best performance in part 1 are selected for EUV testing in the second part.

2.1 Chemical outgassing test

Chemical outgassing or hydrogen induced outgassing (HIO) is a process where activated hydrogen species that exist in EUV-induced hydrogen plasma react with (absorber) elements and form volatile hydrides. When these volatile hydrides come in contact with EUV mirror optics, such as a mirror or the reticle, they may deposit on the optical surfaces and cause irreversible reflectivity loss of the scanner.

In the chemical outgassing test the absorber materials were exposed to hydrogen radicals. These radicals were generated with a hot tungsten filament. A ruthenium coated witness plate was present near the absorber material to mimic an EUV

mirror surface. Chemical outgassing is quantified with ex-situ XPS analysis of the witness plate after the exposure. If absorber elements are present on the witness plate, chemical outgassing of the absorber has occurred.

Two chemical outgassing tests were performed, for PtMo and TaCo alloys. RuTa was not tested since these elements are part of the current standard reticles that are widely used in the EUV scanners. The Pt₂Mo contains the same elements as PtMo, the effect of the different stoichiometry is not expected to impact the chemical outgassing results for this absorber. The PtMo sample was tested without a Mo-Si multilayer. Chemical outgassing is a surface related process, therefore a multilayer was not required.

In the chemical outgassing test the hydrogen radical flux is higher than in the EUV scanner to accelerate the test conditions. In the 20 hours exposure the absorber materials receive at least 70% of the hydrogen radical dose of what the NXE and EUV lithography system (300 W source) produces in about one year at reticle level. The test starts with a background test without absorber material present to validate the cleanliness of the setup itself. After the background is validated, the chemical outgassing test is performed with the absorber material.

Figure 2 and 3 show the XPS spectra as measured on the witness plate. Both the background test spectra (red line) and the chemical outgassing test spectra (orange/yellow line) are plotted. The spectra were normalized to provide a good overlay. The two vertical dotted lines indicate the positions where the peaks of the absorber elements would appear if they were present. Ta, Co, Pt or Mo peaks were not measured. We thus conclude that the TaCo and PtMo alloys did not show chemical outgassing.

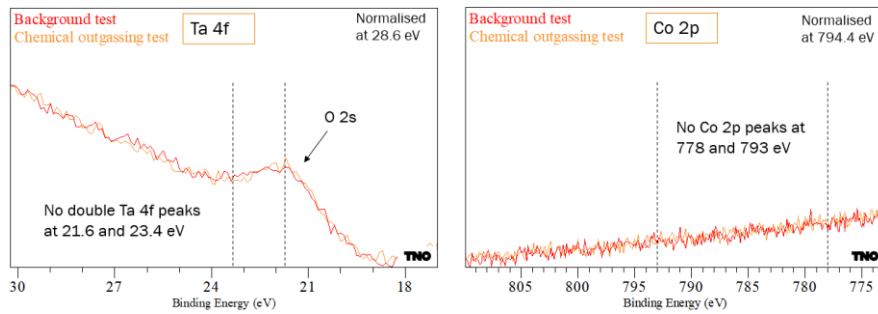


Figure 2: XPS analysis of the Ru witness plate after the chemical outgassing test of TaCo.

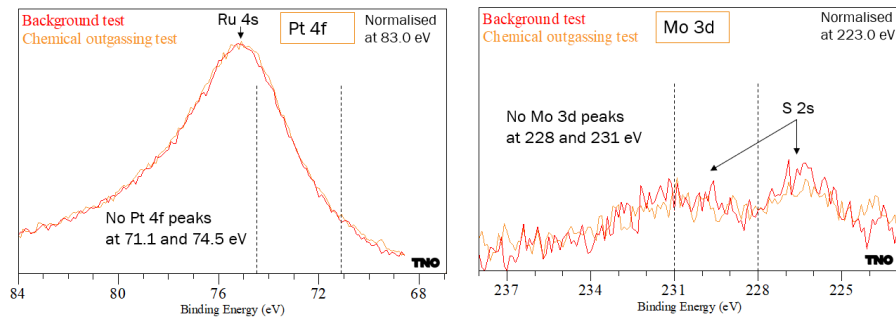


Figure 3: XPS analysis of the Ru witness plate after the chemical outgassing test of PtMo.

2.2 Hydrogen plasma resistance test

The activated hydrogen species, ions and radicals, that exist in EUV-induced hydrogen plasma may penetrate into the absorber layer(s). Recombination to molecular hydrogen underneath the absorber layer can lead to a pressure build up, inflation of the absorber layer (blister formation) and finally into delamination of layers if the blister ruptures. Blister formation will affect the imaging performance and delamination will also result in particle contamination that may re-deposit on the mirrors or the reticle itself leading to reflectivity loss and printable defects.

A shielded microwave source was used for the hydrogen plasma test. The absorber materials were exposed to 24 hours of hydrogen plasma. The test is performed at 1 kW peak source power and a hydrogen pressure of 0.36 mbar. Duty cycling of the plasma and water-cooling of the sample stage during exposure are used to keep the sample temperature below 70 °C. The ion flux in the test is set higher than in the scanner to accelerate the test conditions. The test duration corresponds with an EUV exposure in the scanner of at least 250 thousand wafers.

The plasma test was performed on all four absorber materials (PtMo, Pt₂Mo, TaCo and RuTa alloys) in one run. After exposure samples were analyzed with a light microscope (LM) and a scanning electron microscope (SEM). Figure 4 shows SEM images of the center of each absorber sample before and after the exposure. The 'Low Vacuum Detector' (LVD) was used for SEM imaging. This detector captures secondary electrons which yields primarily topographical information of the surface. The slight color difference between the pre and post images is not due to the exposure but a result of the SEM settings that were used. No plasma-induced defects were observed in the center of all four absorber samples.

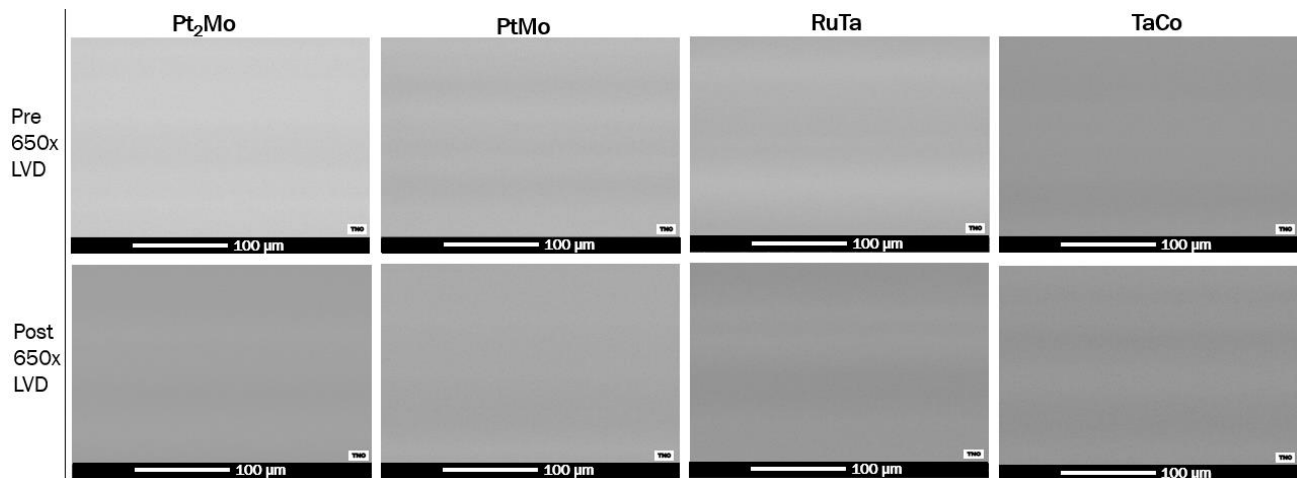


Figure 4: LVD SEM images in the center of the four absorber samples before (top row) and after (bottom row) the hydrogen plasma resistance test.

Additionally, the complete surface of all samples was inspected with a light microscope at 100x magnification. Besides some minor (particle) contamination no blistering or delamination was observed for the Pt₂Mo, PtMo and RuTa alloys.

The TaCo alloy sample showed two features near the center of the sample, as observed with the light microscopy, see Figure 5. SEM imaging was used for further analysis. The large feature was confirmed to be a closed blister. In the center of the blister some contamination or coating artefact was observed. It is likely this caused the blister formation rather than an intrinsic effect of the absorber material. Blistering related to the intrinsic properties of an absorber material is expected to result in large surface areas fully covered with blisters, rather than one or two single, isolated blisters. The other small feature could not be traced back with the SEM. The observed blister shows that cleanliness of the absorber surface is important to prevent contamination induced defects.

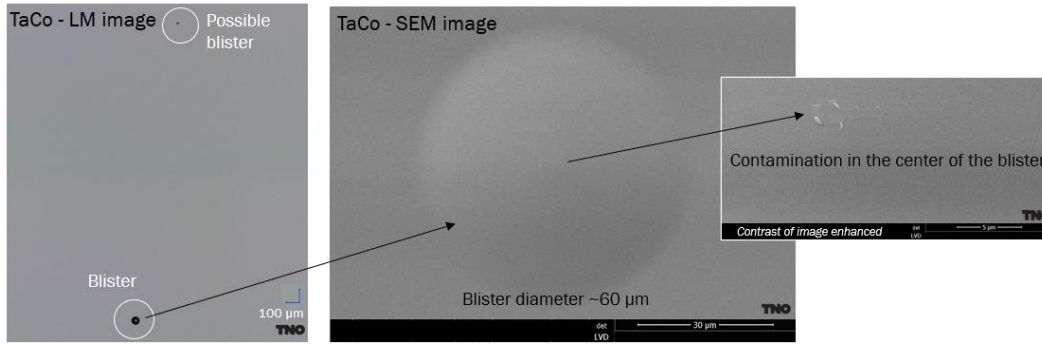


Figure 5: LM and SEM-LVD images of the two features found on the TaCo sample after hydrogen plasma exposure.

The blister on the TaCo alloy is not considered a relevant damage with respect to the assessment of the intrinsic absorber material as it is likely caused by an external factor. All four materials are thus considered resistant to hydrogen plasma in a scanner for at least the equivalent exposure time of 250 thousand wafers and are therefore all candidates for the EUV exposure test.

3. COMPATIBILITY ASSESSMENT – PART 2 – EUV TEST

Part two of the assessment is an EUV exposure in the EBL2 facility at TNO^[7]. Absorber materials are exposed to both EUV light and associated EUV induced plasma containing hydrogen radicals and hydrogen ions. The test conditions are accelerated with respect to the EUV scanner conditions. The EBL2 EUV exposure of 6 hours represents about 1-2 months of EUV dose (at least 150 thousand wafers) in a NXE or EXE system with a 300 W source. The acceleration is performed by increasing the EUV peak intensity to 450 mW/mm² in a static exposure setting. A total peak dose of 9.6 kJ/mm² was applied at 3 kHz EUV source pulse repetition rate. The sample holder was cooled to obtain an estimated steady state sample temperature of 60 °C ± 5 °C in the EUV spot.

We aim for a realistic balance between EUV intensity and plasma conditions in our test. This balance can be tuned with the hydrogen pressure during exposure, because the plasma-dose depends on pressure while the EUV dose does not. A pressure of 0.4 mbar was chosen for this test, since the plasma intensity at a more realistic pressure range of 0.01-0.1 mbar^[8] was considered too low. This hydrogen pressure results in a total ion dose equivalent to an EUV exposure of a least 150 thousand wafers. In the hydrogen environment contaminant gasses H₂O and N₂ were added.

Two absorber materials were selected to be exposed to EUV: RuTa and PtMo alloys. The samples were not patterned. Three samples of each absorber material were mounted on the sample holder for the EUV exposure, see Figure 6.

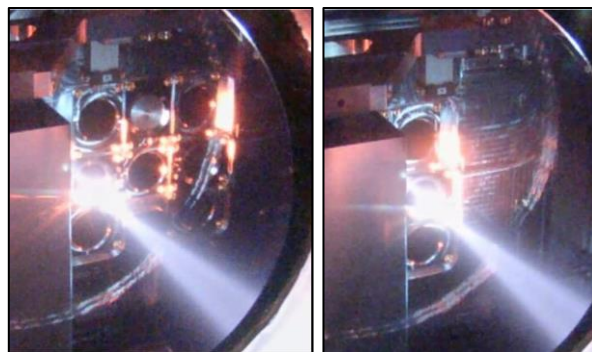


Figure 6: Left picture: EUV exposure of RuTa absorber material. Above and below the EUV exposed RuTa sample are two other RuTa samples that are only exposed to EUV induced plasma (no direct EUV light). On the right, next to the exposed sample, is the ruthenium witness sample. Right picture: EUV exposure of PtMo absorber material.

One sample was directly exposed to the EUV beam and two additional samples were positioned adjacent to the exposed sample. Their purpose is to maximize the surface area of the absorber material available for interactions with EUV induced hydrogen plasma. A ruthenium coated witness sample is present to assess chemical outgassing and redeposition.

3.1 Imaging ellipsometry

The EBL2 setup is equipped with an in-situ imaging ellipsometer to monitor the surface-state of test samples during exposure. The ellipsometer is operated at a wavelength of 640 nm, has an imaging-resolution of approximately 0.1 mm and is sufficiently sensitive to detect subtle changes of less than one atomic monolayer (e.g. removal of adsorbed water, oxygen and carbon in EUV-plasma). Quantitative interpretation at this level is extremely challenging and beyond the scope of this publication. This would require detailed optical models of the sample surface including adsorbate(s). The ellipsometry data is not used to assess the absorber material on scanner compatibility, this is done with LM and SEM analysis of the surface, see paragraph 3.3. Our main goal was to generate qualitative data on the time-dependence of changes in the sample (i.e. to clarify when a local surface change appeared).

We used a variant of nulling ellipsometry: detuned nulling. We acquire two camera images near the nulling setpoint (defined before exposure), with a waveplate rotation of plus and minus 8 degrees with respect to null position. These two images are subtracted and this yields an image where each pixel value is linear to the local change in delta (i.e. the phase difference between the reflected p- and s- polarized light). Such images are acquired with a time-resolution of approximately one minute, and we show some examples in this work to qualitatively illustrate the surface changes that occurred. Imaging ellipsometry was performed continuously during the exposure at the position of the EUV spot.

RuTa sample: An imprint of the EUV spot appeared on the ellipsometry camera after approximately two minutes of EUV exposure. Most likely this is due to local carbon removal. Therewith two small spots becomes visible. After eight minutes the imprint of the EUV spot is fading, while another spot appeared in the EUV spot area. We analyzed these spots with light microscopy and SEM, see paragraph 3.3. Further changes in the EUV spot were not observed during the exposure. See Figure 7 for some key images.

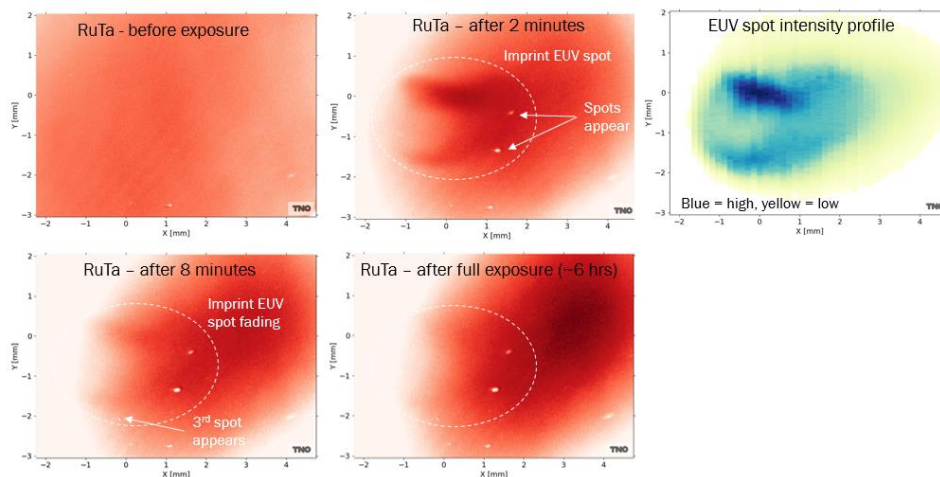


Figure 7: Left four images: Imaging-ellipsometry data acquired during the EUV exposure of RuTa using our ‘detuned nulling’ approach. All four images are shown with the same color-scale range (max – min) and thus contrast is comparable. Absolute signals/colors are not comparable between images though. Right image: EUV spot intensity profile.

PtMo sample: The EUV spot area appears slightly darker than outside the EUV spot area after about two minutes of exposure, but the shape of the EUV spot cannot be distinguished. The subtle change is probably due to local carbon removal. After the full exposure time no defects are visible in the EUV spot area, see Figure 8.

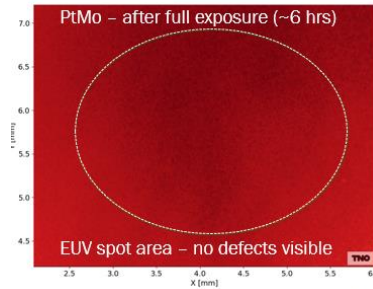


Figure 8: Imaging-ellipsometry data acquired after the EUV exposure of PtMo using our ‘detuned nulling’ approach.

3.2 XPS

The EBL2 is equipped with in vacuo sample transfer from the EUV exposure chamber to the XPS measurement system. This allows transfer of all test samples to XPS for surface analysis without breaking vacuum. Atmospheric effects of the sample surface, e.g. oxidation, are thus eliminated and the XPS results give a good representation of the sample surface conditions after EUV exposure.

The XPS results of the ruthenium witness plate did not show Ta for the RuTa absorber and no Pt or Mo for the PtMo absorber material. These results further strengthen the previous conclusion from the chemical outgassing test without EUV.

XPS measurements were also performed on the exposed absorber samples itself. This is an additional analysis that is not required for the compatibility assessment. The graphs show three XPS spectra, before the exposure (‘pre’), after the EUV exposure in the high EUV intensity area (‘in EUV spot’) and 5 mm from the EUV spot (‘outside EUV spot’) where the surface is only exposed to EUV-induced plasma. The XPS measurement depth is up to 10 nm, so the XPS detects only the top surface and not the bulk material.

RuTa sample: the Ru is not oxidized before and after the exposure, see Figure 9. Since the XPS measurements after exposure were performed in vacuo, the oxygen-fraction of the elements at the surface stayed low after EUV exposure (re-oxidation does not occur). As a result, the peaks in the spectra for other elements become larger than in the pre measurement. The Ta is about 50% oxidized before the exposure. After the exposure the Ta is partly reduced, about 20% is still oxidized in the EUV spot and outside the EUV spot about 26%, see Figure 10. In the XPS maps the outline of the EUV spot is clearly visible.

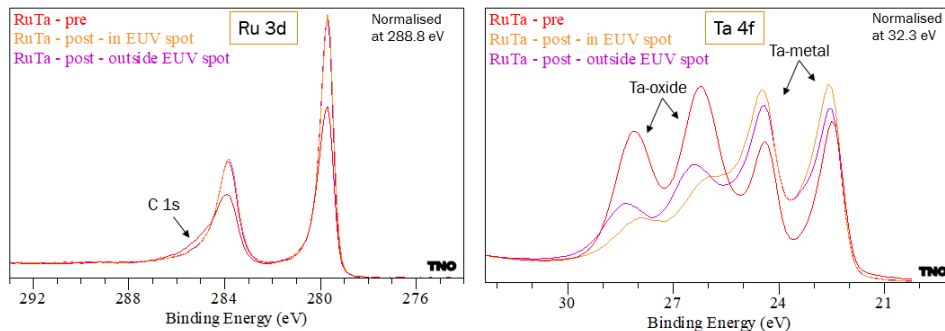


Figure 9: XPS spectra of the RuTa sample before and after EUV exposure.

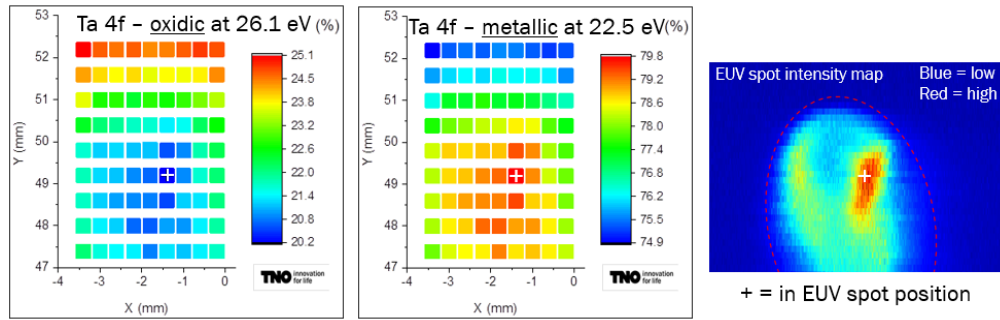


Figure 10: XPS maps of the EUV spot after the EUV exposure showing the splitting of the Ta 4f peak in the oxidic part (left) and metallic part (center). Together, the values in the maps add up to 100%. The right image is the corresponding EUV intensity map.

PtMo sample: The Pt before and after exposure is in the metallic state, no changes are observed, see Figure 11. The Mo is about 36% oxidized before the exposure and after exposure the Mo is fully reduced to the metallic state. There was no imprint of the EUV spot visible in the XPS maps.

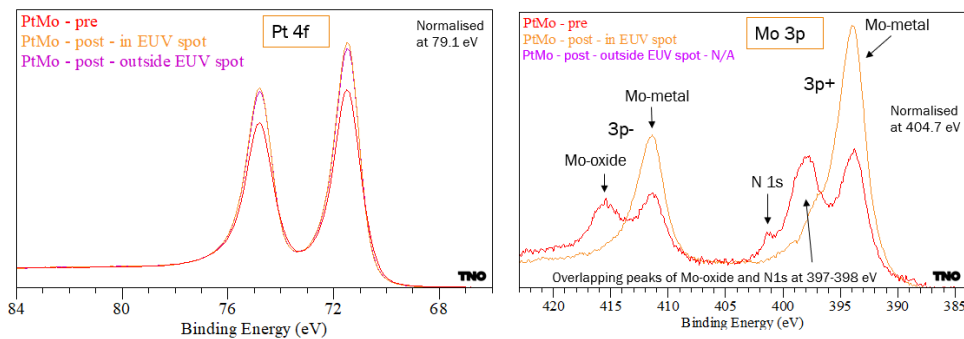


Figure 11: XPS spectra of the PtMo sample before and after EUV exposure.

The reduction of elements from an oxidic state to a metallic state is attributed to the hydrogen plasma created by interaction of EUV radiation with hydrogen gas. This most likely also occurs in the EUV scanner. It is reported that carbon and oxidation on the reticle surface slowly disappear during EUV exposure after a new reticle is loaded^[9]. This was measured on a Ta-based absorber. Upon re-exposure to atmospheric conditions the elements on the surface will (partly) re-oxidize and thus this effect can be expected to repeat for each reticle (re)load.

3.3 Light microscopy and SEM

SEM imaging was performed to assess potential EUV-induced damage, like blistering or delamination, of the absorber surface. The high EUV intensity areas were mapped with SEM at a 518x magnification and at several positions at higher resolutions, see Figure 12 and 13. The single SEM images in the map have a Horizontal Field Width (HFW) of 400 μm . In the high EUV intensity area the absorber surfaces were fully intact, blistering or delamination was not observed. The encircled particle on the RuTa sample was already present before the exposure.

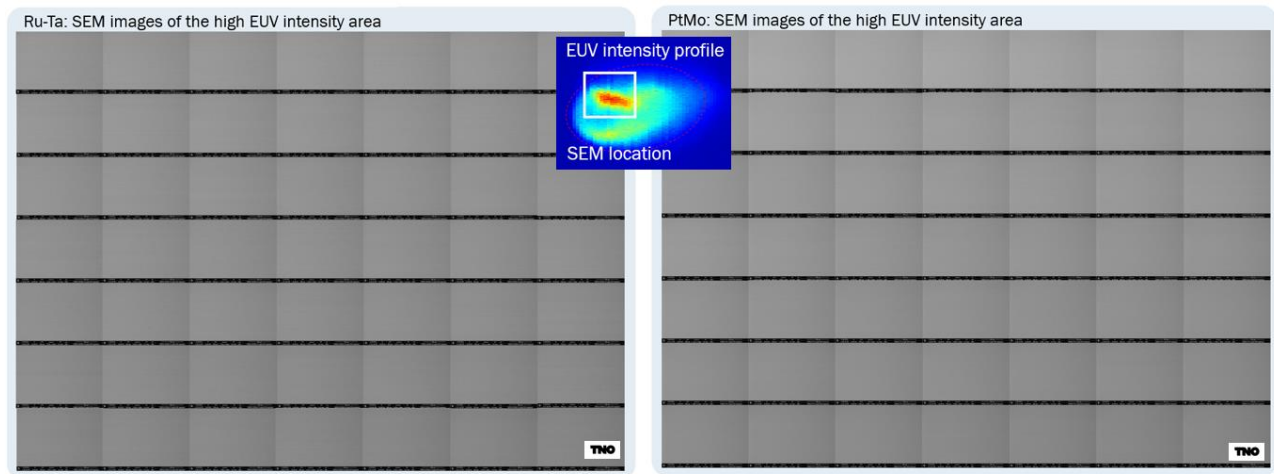


Figure 12: SEM imaging with ‘Gaseous Analytical Detector’ (backscatter electrons) of the high EUV intensity areas of RuTa (left) and PtMo (right). In the center is the SEM map location indicated on a the EUV intensity profile.

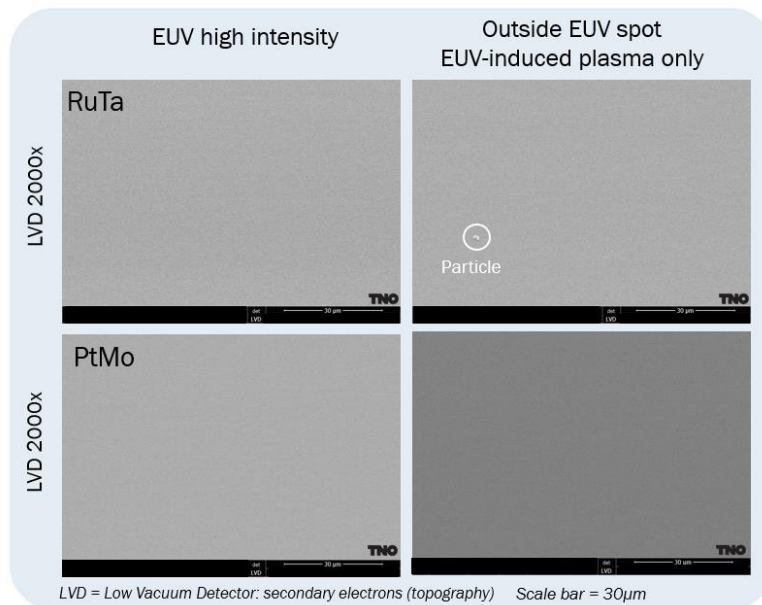


Figure 13: SEM LVD imaging of RuTa and PtMo at high resolution (2000x magnification) after EUV exposure. Positions are in the high EUV intensity area (left) and outside the EUV spot where there is only EUV-induced plasma (right). The color difference between the PtMo images is not due to the exposure but a result of the SEM settings that were used.

In the lower EUV intensity area on the RuTa alloy, three blister locations were found, see Figure 14. Each one of them shows dark spots in between the blisters and a sharp outline surrounding the blister location. This is an indication that the blister process is likely to be provoked by particle contamination or a coating defect. For position 2 and 3 we were able to verify with the light microscopy measurements before the EUV exposure that the black spots and/or the outline were already present.

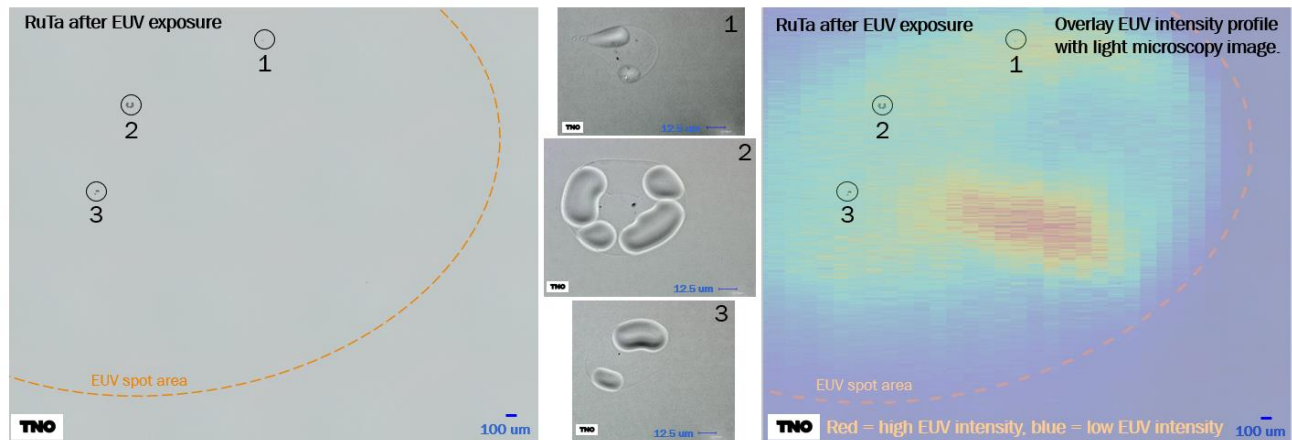


Figure 14: RuTa after EUV exposure; left: light microscopy image with indications of the blister locations; center: light microscopy images at higher magnifications of the three blister locations; right: overlay of the EUV intensity profile on top of the light microscopy image, overlay accuracy up to ~0.5 mm.

In the lower EUV intensity area on the PtMo alloy, one blister location was found, see Figure 15. Similar to the RuTa, dark spots are in between the blisters and a sharp outline is surrounding the blister location. In the light microscopy data before the EUV exposure there were no images of the blister location with sufficient resolution to verify the condition of the absorber surface, but it is assumed some contamination or coating defect was also present before the exposure.

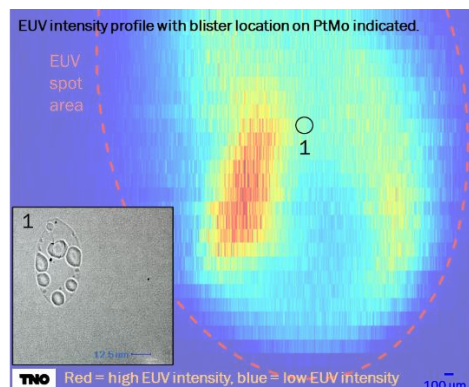


Figure 15: EUV intensity profile with blister location on PtMo indicated. Inset: light microscopy image of the blisters.

Both the RuTa and PtMo alloy showed good performance during EUV exposure. Relevant surface defects and chemical outgassing were not observed. The few observed blisters in the lower EUV intensity areas are likely provoked by particle contamination or coating defects.

To finalize the compatibility assessment a test would be required with a patterned reticle that is manufactured similar to reticles that are going to be used for exposures in the EUV scanner. This reticle has a full multilayer coating and full absorber stack on a low thermal expansion material or a quartz substrate and a dedicated pattern.

4. CONCLUSIONS

Four candidate reticle absorber materials have been evaluated for compatibility with conditions during use in an EUV scanner: TaCo, RuTa, PtMo and Pt₂Mo alloys. The tested materials, TaCo and PtMo, did not show chemical outgassing. RuTa and Pt₂Mo were not tested, because based upon their elemental composition chemical outgassing is not expected. All four materials were resistant to a hydrogen plasma dose equivalent to an EUV exposure of at least 250 thousand wafers. An EUV exposure, equivalent to at least 150 thousand wafers, was performed on the RuTa and PtMo alloys. Both materials showed good performance during the EUV exposure. No relevant surface defects were observed and no chemical outgassing was measured. The few observed blisters in the low EUV intensity areas are likely provoked by particle contamination or coating defects.

All four absorber materials, TaCo, RuTa, PtMo and Pt₂Mo alloys performed well in the compatibility tests that were executed, see Table 1 for an overview. Not all compatibility tests could be performed on each absorber material within the scope of our project. Further testing would be needed to complete the compatibility assessment, including an EUV exposure on a patterned reticle with the novel absorber material. Since compatibility with the EUV scanner is only one of the requirements for novel absorber materials, it is essential to conduct also research on the other requirements, like imaging performance, to develop suitable novel absorber materials for high-NA EUV scanners.

Table 1: Overview of the performed EUV compatibility tests and results.

Absorber material	Coating details (on Si wafer substrates)	Multilayer	Patterned	Test			
				1 - Molecular Outgassing ¹	2 - Chemical outgassing	3 - Hydrogen plasma	4 - EUV exposure
AttPSM candidates							
PtMo	[Mo/Si] ¹⁰ , Ru, PtMo	10 bilayers	No	Not tested	√ ²	√	√
Pt ₂ Mo	[Mo/Si] ¹⁰ , Ru, Pt ₂ Mo	10 bilayers	No	Not tested	Not tested ³	√	Not tested
RuTa	[Mo/Si] ⁴⁰ , Ru, RuTa	40 bilayers	No	√	Not tested ³	√	√
Binary (high-k) mask candidate							
TaCo	[Mo/Si] ⁴⁰ , Ru, TaCo	40 bilayers	No	Not tested	√	√	Not tested

¹ The molecular outgassing test was only performed on the RuTa sample, the results were within the requirements for reticle outgassing.

² Performed on PtMo absorber sample without a multilayer.

³ Chemical outgassing test is not performed, but based upon the elemental composition no chemical outgassing is expected.

ACKNOWLEDGEMENTS

This project has received funding from the ECSEL Joint Undertaking (JU) under grant agreement No 783247. The JU receives support from the European Union's Horizon 2020 research and innovation program and Netherlands, Belgium, Germany, France, Austria, United Kingdom, Israel, Switzerland.



REFERENCES

- [1] Jetske Stortelder, Arnold Storm, Veronique de Rooij-Lohmann, Chien-Ching Wu, Willem van Schaik, "Compatibility assessment of novel reticle absorber materials for use in EUV lithography systems.," Proc. SPIE 10957, Extreme Ultraviolet (EUV) Lithography X, 1095713 (2019); <https://doi.org/10.1117/12.2513887>
- [2] Meiyi Wu, Devesh Thakare, Jean-François de Marneffe, Patrick Jaenen, Laurent Souriau, Karl Opsomer, Jean-Philippe Soulié, Andreas Erdmann, Hazem Mesilhy, Philipp Naujok, Markus Foltin, Victor Soltwisch, Qais Saadeh, Vicky Philipsen, "Mask absorber for next generation EUV lithography" Proc. SPIE 11517, Extreme Ultraviolet Lithography 2020, 1151706 (20 October 2020); doi: 10.1117/12.2572114.
- [3] Meiyi Wu, Devesh Thakare, Jean-François de Marneffe, Patrick Jaenen, Laurent Souriau, Karl Opsomer, Jean-Philippe Soulié, Andreas Erdmann, Hazem M. S. Mesilhy, Philipp Naujok, Markus Foltin, Victor Soltwisch, Qais Saadeh, and Vicky Philipsen, "Study of novel EUVL mask absorber candidates," Journal of Micro/Nanopatterning, Materials, and Metrology 20(2), 021002 (3 May 2021). <https://doi.org/10.1117/1.JMM.20.2.021002>
- [4] Frank Scholze, Christian Laubis, Kim Vu Luong, Vicky Philipsen, "Update on optical material properties for alternative EUV mask absorber materials," Proc. SPIE 10446, 33rd European Mask and Lithography Conference, 1044609 (28 September 2017); <https://doi.org/10.1117/12.2279702>
- [5] Andreas Erdmann, Hazem S. Mesilhy, Peter Evanschitzky, Vicky Philipsen, Frank J. Timmermans, and Markus Bauer "Perspectives and tradeoffs of absorber materials for high NA EUV lithography," Journal of Micro/Nanolithography, MEMS, and MOEMS 19(4), 041001 (1 October 2020). <https://doi.org/10.1117/1.JMM.19.4.041001>
- [6] Claire van Lare, Frank Timmermans, and Jo Finders "Mask-absorber optimization: the next phase," Journal of Micro/Nanolithography, MEMS, and MOEMS 19(2), 024401 (6 May 2020). <https://doi.org/10.1117/1.JMM.19.2.024401>
- [7] Herman Bekman, Michael Dekker, Rob Ebeling, Jochem Janssen, Norbert Koster, Joop Meijlink, Freek Molkenboer, Kyri Nicolai, Michel van Putten, Corné Rijnsent, Arnold Storm, Jetske Stortelder, Chien-Ching Wu, Rory de Zanger, "EBL2 an EUV (Extreme Ultra-Violet) lithography beam line irradiation facility," Proc. SPIE 11147, International Conference on Extreme Ultraviolet Lithography 2019, 1114706 (26 September 2019); <https://doi.org/10.1117/12.2536531>
- [8] Mark van de Kerkhof, Ernst Galutschek, Andrei Yakunin, Selwyn Cats, Christian Cloin, "Particulate and molecular contamination control in EUV-induced H₂-plasma in EUV lithographic scanner", Proc. SPIE 11489, Systems Contamination: Prediction, Control, and Performance 2020, 114890K (23 August 2020); doi: 10.1117/12.2569997
- [9] Rik Jonckheere, Chien-Ching Wu, Veronique de Rooij-Lohmann, Dorus Elstgeest, Henk Lensen, Philipp Honicke, Michael Kolbe, Victor Soltwisch, Claudia Zech, Frank Scholze, Remko Aubert, Vineet Vijayakrishnan Nair, Eric Hendrickx, "Study of EUV reticle storage effects through exposure on EBL2 and NXE", Proc. SPIE 11517, Extreme Ultraviolet Lithography 2020, 115170Z (2020); doi: 10.1117/12.2573125.